Journal of Applied Polymer Science

Development of Lightweight Thermoplastic Composites Based on Polycarbonate/Acrylonitrile-Butadiene-Styrene Copolymer Alloys and Recycled Carbon Fiber: Preparation, Morphology, and Properties

Guotao Yan, Xiaodong Wang, Dezhen Wu

State Key Laboratory of Organic-Inorganic Composite Materials, School of Materials Science and Engineering, Beijing University of Chemical Technology, Beijing, China

Correspondence to: X. Wang (E-mail: wangxdfox@yahoo.com.cn)

ABSTRACT: Thermoplastic composites of polycarbonate (PC)/acrylonitrile–butadiene–styrene copolymer (ABS) alloys reinforced with recycled carbon fiber (RCF) were prepared by melt extrusion through a twin-screw extruder. The RCF was first cleaned and activated with a concentrated solution of nitric acid and was then surface-coated with diglycidyl ether of bisphenol A as a macromolecular coupling agent. Such an approach is effective to improve the interfacial bonding between the fibers and the PC/ABS matrix. As was expected, the reinforcing potential of the RCF was enhanced substantially, and furthermore, the mechanical properties, heat distortion temperature, and thermal stability of PC/ABS alloys were significantly improved by incorporating this surface-treated RCF. The composites also obtained a reduction in electrical resistivity. The morphologies of impact fracture surfaces demonstrated that the RCF achieved a homogeneous dispersion in the PC/ABS matrix due to good interfacial adhesion between the fibers and the matrix. In addition, the introduction of RCF into PC/ABS alloys also resulted in an increase in the storage moduli of the composites but a decrease in the loss factors. It is prospective that, with such good performance in mechanical data, heat resistance, and electrostatic discharge, the RCF-reinforced PC/ABS composites exhibit a potential application in industrial and civil fields as high-performance and lightweight materials. © 2013 Wiley Periodicals, Inc. J. Appl. Polym. Sci. 129: 3502–3511, 2013

KEYWORDS: composites; polycarbonates; fibers; mechanical properties; recycling

Received 29 October 2012; accepted 30 January 2013; published online 28 February 2013

DOI: 10.1002/app.39105

INTRODUCTION

The plastic alloys based on polycarbonate (PC) and acrylonitrile–butadiene–styrene copolymer (ABS) are a class of well-known commercial engineering plastic blends with good comprehensive properties due to a unique combination of the high thermal stability and impact toughness of PC and the easy processability and economical benefits of ABS.[1,2] PC/ABS alloys have been widely used in automotive, electrical, and electronic fields covering the personal consumption and industrial production.[3–5] Although promising, however, insufficient mechanical strength and heat resistance of the PC/ABS alloys have often hindered their potential application in a broad range of industrial fields.[6,7] Therefore, the development of carbon-fiber-reinforced PC/ABS alloys over the past years has brought a great competitor to traditional glass-fiber-reinforced PC/ABS composites. Compared to the PC/ABS alloys reinforced with glass fiber or the other inorganic fibers, the carbon-fiber-reinforced PC/ABS composites feature the improved tensile strength and modulus, flexural strength and modulus, and retention of physical properties in humid environments.[8,9] They also offer a reduced coefficient of thermal expansion, lower mold shrinkage, increased thermal conductivity, improved creep resistance, superior wear resistance, and outstanding toughness.[10] Moreover, such composites can gain the high thermal resistance to the heat generated from the engine, superior mechanical properties against external vibrations and impacts, good electromagnetic interference (EMI) shielding characteristics, and lightweight.[9,11,12] Considering that the automotive industry has made great efforts to develop lightweight vehicles for the achievement of low fuel consumption, the carbon-fiber-reinforced engineering plastics as substitute materials have been developed for the manufacture of many automotive parts to replace conventional steel parts.[13,14] These features have made the carbon-fiber-reinforced PC/ABS composites a good candidate for the manufacture of many automotive parts and devices. Huang and Wu[15] reported an investigation on PC/ABS/nickel-coated carbon-fiber composites and found that this composite material achieved good EMI shielding effectiveness and high

mechanical strength as well as good processability. Jeon et al.[5] developed a series of PC/ABS based composites with a mixture of carbon fiber, metal fiber, and glass fiber. These composites obtained a good balance of mechanical stiffness and strength, high EMI shielding effectiveness, good injection moldability, and reduced weight, and therefore, they were adapted for the manufacture of complex-shaped car audio chassis.

It is no doubt that carbon fiber is an excellent reinforcement material for the most of polymer-based composites and has created many structural composite materials.[16–18] Carbon-fiber-reinforced composites are now used in a widening range of applications and in growing content in most of them. The aircraft industry is an impressive example, with the new Boeing 787 and Airbus A350 having up to 50% of their weight in carbon-fiber-reinforced composites and military aircraft showing a similar trend.[19] According to statistics of "The Carbon Fibre Industry Worldwide 2008–2014" published by Materials Technologies Publications, UK, the worldwide demand for carbon fiber reached approximately 35,000 tones in 2008, and this number is expected to double by 2014, representing a growth rate of over 12% per year.[19] However, as the worldwide amount of carbon fiber used for composite materials grows, there is concern about the potential tonnage of waste from manufacturing processes and end-of-life products. The waste related to carbon-fiber-reinforced products will quickly reach a significant level to become an important environmental issue since such products are not biodegradable. In addition, the raw carbon fiber is extremely expensive because of the high consumption of energy in its manufacture.[20,21] Such a high consumption of energy also keeps away from the trend of green chemistry, and therefore, manufacturers will need to identify ways to comply with legislation on sustainability.[22] In recent years, there is a strong interest in developing processes for recovering and recycling of carbon fiber from waste materials. Several methods have been developed for the carbon-fiber recovery from carbon-fiber-reinforced thermoplastic and thermoset waste. A recovery process for composite materials has been developed based upon a fluidized bed process.[23,24] The process provides high quality, clean fibers with good mechanical property retention.[25] Consequently, it maybe arise up new interest and opportunity to study the reusing of the waste carbon fiber recycled.[26–29] A few studies have been reported on the thermoplastic composites with recycled carbon fiber (RCF). Akonda et al.[30] studied the reinforcing effect of RCF on polypropylene and showed that, for composite specimens containing 27.7% RCF by volume, the average values obtained for tensile and flexural strength were 160 and 154 MPa, respectively. McNally et al.[31] investigated the polyethylene-based composites with RCF prepared through melt compounding and found that both the tensile strength and Young's modulus increased with increasing RCF loading. Wong et al.[32] reported the development of an EMI shielding material using RCF, which was transformed to a non-woven veil molded into a thermoplastic plaque. It was found that the shielding effectiveness and performance increased with veil areal densities as well as the degree of fiber dispersion. Wong et al.[33] also investigated the effect of coupling agents on reinforcing potential of RCF for polypropylene-based composite. The results showed that the reinforcing potential of the recycled fiber was increased by improving the interfacial adhesion between the fiber and matrix with the addition of maleic anhydride-grafted polypropylene coupling agents. Pimenta and Pinho[34] investigated the effect of recycling on the mechanical response of carbon fiber and its composites and answered the question how good can the performance of recycled composites be. It was convinced that, with such mechanical properties improved, the thermoplastic composites made from RCF can be used as low cost materials for many nonstructural applications, and the recovery and reusing of RCF to reinforce the engineering plastics can offer sound economic benefits.

In this study, we employed the carbon fiber recycled from the waste thermosetting resin-based composites to prepare the RCF-reinforced PC/ABS thermoplastic composites via a simple melt extrusion using a conventional twin-screw extruder. An intensive investigation was also carried out focusing on the mechanical properties, heat resistance, electrical conductivity, morphology, and thermal stability, so that a high-performance and lightweight composite material can be developed based on the results of this work. As aforementioned, carbon-fiber-reinforced PC/ABS composites have showed the superiority in outstanding mechanical properties as well as their lightweight characteristics. Therefore, it is prospective that the importance and novelty of RCF reused for reinforcing PC/ABS composites will offer a cost-effective means to achieve the properties similar to raw carbon fiber and also provide high-performance and lightweight composite materials that would find widespread use in automotive, electric and electronic, and civil engineering applications.

EXPERIMENTAL

Materials

PC (Panlite® L-1250Y) with a specific gravity of 1.2 and a melt flow index of 9.6 g/10 min was purchased from Teijin Chemicals, Tokyo, Japan. ABS resin (Polylac® PA-757) with a specific gravity of 1.05 and a melt flow index of 1.8 g/10 min was purchased from Chi Mei Corp., Tainan, Taiwan. The RCF was kindly supplied by Weiyuan Chemical Fibre Co., Xiamen, China. It was recycled from the waste carbon-fiber-reinforced thermosetting products through the thermooxidative decomposition upon fluidized bed process to remove the organic resins. Diglycidyl ether of bisphenol A (DGEBA), used as a coupling agent for the surface treatment of RCF, was commercially obtained from BlueStar New Chemical Materials Co., Wuxi, China.

Preparation of Composites

The RCF was firstly immersed in a concentrated solution of nitric acid for 2 h to clean and polarize the fiber surfaces. After washed to neutrality with deionized water, the activated RCF was further surface-treated with a solution of DGEBA in acetone at a concentration of 8 wt % for 5 h. Then, the RCF with the saturated absorption of the coupling agent was baked under a vacuum at 90°C for 2 h.

The raw PC and ABS were dried at 85°C for 12 h to ensure the moisture content is enough low to prevent degradation. The PC/ABS composites with various weight percent of

surface-treated RCF were blended through melt extrusion using a corotating twin-screw extruder (d = 30 mm, L/D = 40, Nanjing Rubber & Plastics Machinery Plant Co., Nanjing, China) with a screw configuration adapted to fiber/thermoplastic reinforcement. The temperatures along the barrel from feeding zone to die were set at 240, 245, 255, 260, 260, 255, 250, and 245°C, and the rotating speed of the screw was 180 rpm. The extrusion parameters were slightly varied from one composition to another. The melting extrudate was cooled in a water bath and subsequently pelletized. The resulted pellets were dried under vacuum at 85°C overnight and then were stored in the sealed aluminum foil bags.

Characterization

Mechanical Performance Test. All the samples were dried at 110°C for 8 h prior to injection molding and were then injection-molded into the test bars with the different shapes required for mechanical and heat-resistant measurements. The tensile and flexural properties were measured with a SANS CMT-4104 universal testing machine using a 10,000 N load transducer according to ASTM D-638 and D-790 standards, respectively. Notched Izod impact strength was measured with a SANS ZBC-1400A impact tester according to ASTM D-256 standard. The thickness of notched Izod impact bars was 1/8 in., and impact energy was 2.75 J. All the tests were done at room temperature, and the values reported reflected an average from five tests.

Heat Distortion Temperature Test. The specimens for heat distortion temperature (HDT) testing were first prepared via injection molding. The HDTs of virgin PC/ABS alloys and their composites with various RCF loadings were measured with a SANS ZWK-1000 Heat distortion & Vicat softening temperature testing machine under a load of 1.82 MPa according to ASTM D-648 standard, and all the HDTs represented the average values over the five measurements.

Electrical Resistivity Test. The specimens for volume resistivity and surface resistivity tests were prepared through injection molding. The surface resistivity and volume resistivity of the RCF-reinforced PC/ABS composites were measured with a PC68 digital teraohmmeter under a voltage of 500V according to ASTM D-257 standard, respectively. The data reported were obtained by the average values of the five tests for each sample.

Scanning Electron Microscopy. Scanning electron microscope (SEM) images for the morphologies of RCF surface and fractography of RCF-reinforced PC/ABS composites were taken on a Zeiss Supra 55 SEM. The fracture surfaces obtained from impact test bars after impact measurement were made electrically conductive by sputter coating with a thin layer of gold–palladium alloy. The images were taken in high vacuum mode with 20 kV acceleration voltage and a medium spot size.

Thermogravimetric Analysis. Thermogravimetric analysis (TGA) was carried out in a nitrogen atmosphere using a TA Instruments Q50 thermal gravimetric analyzer. Samples were placed in a platinum crucible, and ramped from room temperature to 700°C at a heating rate of 10°C/min, while a flow of nitrogen was maintained at 50 mL/min.

Dynamic Mechanical Analysis. The dynamic mechanical behaviors of the RCF-reinforced PC/ABS composites were measured on a TA Q-800 dynamic mechanical analyzer under a dual cantilever mode. The test was run during the temperature range from −50°C to 220°C with a heating rate of 5°C/min and a strain amplitude of 10 μm at a frequency of 1 Hz.

RESULTS AND DISCUSSION

Mechanical Properties

The tensile and flexural test results of RCF-reinforced PC/ABS composites are presented in Table I. An intuitive trend of these mechanical properties can be clearly observed with the variation of RCF loading as well as PC/ABS weight ratio. The RCF displays a very significant reinforcing effect on PC/ABS alloys. The introduction of only 5 wt % of RCF can lead to approximate 60% and 35% improvements in tensile and flexural strength, respectively. Such an increasing trend was well maintained with increasing the RCF loading, and the composite achieved an around 150% increase in the two mechanical parameters when 20 wt % of RCF was incorporated. Meanwhile, compared to virgin PC/ABS alloys, their composites with RCF also gained a significant increment by more than five times in tensile and flexural moduli. The significant enhancement in the mechanical parameters of PC/ABS composites is mainly ascribed to good interfacial shear strength between fibers and PC/ABS matrix.[35] As aforementioned, the RCF was surface-treated with DGEBA epoxy resin, which has a similar molecular segment with PC. Therefore, this epoxy coupling agent is thermodynamically miscible with PC, and an interfacial adhesion can be enhanced between the fibers and the matrix by the bridging effect of DGEBA. It is believed that the good interfacial interaction may offer an efficient load transfer to the polymer matrix, and thus, a mechanical interlocking was established between the fibers and matrix. Such a process can prevent the crack growth from passing through the interfacial boundary between the fibers and matrix and make the composites withstand more test stress. As a result, the composites achieved much higher reinforcement effect in comparison with the results previously reported by the literature.[12,15] Herein, the DGEBA macromolecular coupling agent evidently supplied the major bonding effect to enhance the interfacial adhesion between the fibers and the matrix. It is also notable that the RCF exhibited a slight different reinforcing effect on PC/ABS alloys at different weight ratios of PC and ABS. In most case, the lower fraction of ABS the alloys have, the higher mechanical strength and modulus the composites achieved. These results are consistent with the mechanical nature of virgin PC/ABS alloys at different weight ratios.

Table I also reveals the notched Izod impact strength of the composites with different RCF loadings. It is amazingly noted that the RCF also demonstrated a toughening effect on PC/ABS alloys, and incorporating only 5 wt % of RCF resulted in an increase in impact strength by about 30%. Although the impact strength was increasingly improved by increasing the RCF loading, it reached a maximum at 15 wt % of RCF loading and, afterward, decreased with an increasing addition of RCF. Such a decline in impact toughness can be explained by the transformation mechanism of fracture. Generally, there are two factors

Table I. Mechanical Properties of RCF-Reinforced PC/ABS Composites

Sample	Tensile strength (MPa)	Tensile modulus (MPa)	Flexural strength (MPa)	Flexural modulus (MPa)	Notched Izod impact strength (J/m)
PC/ABS (80/20) alloy	55.01 ± 2.65	2818 ± 122	89.08 ± 4.61	2265 ± 212	137.52 ± 5.58
PC/ABS (80/20) alloy + 5 wt % RCF	90.50 ± 3.32	8731 ± 406	140.04 ± 7.35	7158 ± 449	179.24 ± 6.08
PC/ABS (80/20) alloy + 10 wt % RCF	106.13 ± 3.78	12,597 ± 439	161.84 ± 8.28	10,638 ± 503	201.63 ± 7.94
PC/ABS (80/20) alloy + 15 wt % RCF	129.33 ± 3.89	16,974 ± 678	197.69 ± 9.89	13,910 ± 671	249.40 ± 8.97
PC/ABS (80/20) alloy + 20 wt % RCF	135.9 ± 4.04	18,638 ± 745	219.08 ± 10.27	15,218 ± 745	221.58 ± 8.12
PC/ABS (70/30) alloy	57.33 ± 2.49	2754 ± 139	85.87 ± 4.36	2316 ± 160	151.31 ± 6.52
PC/ABS (70/30) alloy + 5 wt % RCF	87.65 ± 3.48	7022 ± 384	132.07 ± 6.48	6335 ± 387	190.33 ± 6.93
PC/ABS (70/30) alloy + 10 wt % RCF	103.97 ± 4.58	9428 ± 377	152.21 ± 8.19	8859 ± 475	194.79 ± 7.24
PC/ABS (70/30) alloy + 15 wt % RCF	127.39 ± 4.99	14,862 ± 594	189.42 ± 8.56	11,764 ± 594	251.50 ± 6.65
PC/ABS (70/30) alloy + 20 wt % RCF	129.74 ± 4.76	16,984 ± 671	196.08 ± 9.76	13,689 ± 679	215.22 ± 7.20
PC/ABS (60/40) alloy	57.15 ± 2.86	2667 ± 106	85.31 ± 3.86	2202 ± 217	154.95 ± 6.47
PC/ABS (60/40) alloy + 5 wt % RCF	87.81 ± 3.51	5977 ± 196	131.75 ± 6.57	5970 ± 273	197.82 ± 5.79
PC/ABS (60/40) alloy + 10 wt % RCF	102.73 ± 4.11	6249 ± 249	154.7 ± 7.12	9161 ± 449	208.16 ± 6.51
PC/ABS (60/40) alloy + 15 wt % RCF	124.86 ± 4.60	12,216 ± 418	173.18 ± 7.69	11,245 ± 584	262.54 ± 8.29
PC/ABS (60/40) alloy + 20 wt % RCF	131.09 ± 4.84	16,654 ± 485	189.91 ± 8.84	12,295 ± 683	219.65 ± 6.34

dominating the impact toughness of fiber-reinforced composites.[36–38] The first one is that new stress concentrations are formed around the fiber ends, area of poor adhesion, and region of fiber aggregation. The second one is that the fibers can enhance the impact toughness through reducing the crack propagation rate by forcing cracks around the fibers. The practical effects of fibers on impact toughness of composites depend on the competition of these two factors. In the case of the RCF-reinforced PC/ABS composites, it is anticipated that the reducing effect of RCF on crack propagation rate of composites dominates crack initiation through forming new stress concentration, and the RCF restricts the crack propagation rate so as to alleviate the fracture of the composites. The energy required to generate a new fracture surface increases with the fiber volume fraction, leading to an increase in impact strength. Furthermore, the fiber pulling-out and fracture, interfacial debonding, and matrix deformation also made contributions to the improvement in impact performance of PC/ABS composites. However, the aggregation of RCF in the case of high loading may occur and, thus, leads to locally destroy the continuity of matrix. This directly results in the decrease of crack propagation capability and the severe matrix deformation. Moreover, the agglomeration of RCF also causes the stress concentration in the PC/ABS matrix and prevents efficient load transfer to the matrix. These results will be confirmed by the morphological observation for the impact fracture surface of RCF-reinforced PC/ABS composites.

Heat Distortion Temperature

HDT is defined as the upper limiting temperature of the dimensional stability of thermoplastics in service without significant physical deformations under a normal load and thermal effect, so it can estimate the elevated temperature performance of engineering materials in service environment and can provide the important information for material design as well.[39] The HDTs of virgin PC/ABS alloys and their composites with various RCT loadings are summarized in Table II. Each of the HDTs reported here represents an average value of five tests. The virgin PC/ABS alloys are observed to give the HDTs ranging from 50 to 57°C at weight ratios from 60/40 to 80/20. Such low HDTs restrict the application of PC/ABS alloys as structural engineering materials in the most industrial and civil areas. It is anticipated that the HDTs have been improved significantly by incorporating RCF into PC/ABS alloys. The composite achieved a high HDT of around 100°C with the addition of only 5 wt % RCF. The composite further exhibited a much higher HDT of about 145°C when 20 wt % of RCF was incorporated. It is evident that the general trend is that the higher RCF loading can impart higher HDT to the composites. As mentioned previously, the high RCF loading in the composites tended to improve the flexural strength and modulus. Many studies reported that the HDT was associated with the mechanical behavior of thermoplastic composites like flexural properties.[40,41] In the HDT measurements, the ability of a thermoplastic material to retain stiffness with increasing temperature is important for the achievement of a high HDT. Generally, the introduction of inorganic fibers or fillers can make it possible for the thermoplastic composites to maintain moderate

Table II. HDTs and Electrical Resistivity of RCF-Reinforced PC/ABS Composites

Sample	HDT (°C)	Volume resistivity (Ω m)	Surface resistivity (Ω)
PC/ABS (80/20) alloy	57.5	2.78×10^{14}	8.9×10^{13}
PC/ABS (80/20) alloy + 5 wt % RCF	102.4	4.7×10^{8}	9.4×10^{8}
PC/ABS (80/20) alloy + 10 wt % RCF	113.6	3.9×10^{7}	6.7×10^{7}
PC/ABS (80/20) alloy + 15 wt % RCF	132.6	3.1×10^{7}	4.1×10^{7}
PC/ABS (80/20) alloy + 20 wt % RCF	147.6	2.7×10^{7}	3.8×10^{7}
PC/ABS (70/30) alloy	53.3	2.45×10^{14}	6.3×10^{13}
PC/ABS (70/30) alloy + 5 wt % RCF	98.33	3.4×10^{8}	6.9×10^{8}
PC/ABS (70/30) alloy + 10 wt % RCF	109.6	3×10^{7}	4.5×10^{7}
PC/ABS (70/30) alloy + 15 wt % RCF	121.6	2.5×10^{7}	3.8×10^{7}
PC/ABS (70/30) alloy + 20 wt % RCF	135.5	2.4×10^{7}	2.9×10^{7}
PC/ABS (60/40) alloy	50.9	1.82×10^{14}	5.1×10^{13}
PC/ABS (60/40) alloy + 5 wt % RCF	97.3	2.4×10^{8}	6×10^{8}
PC/ABS (60/40) alloy + 10 wt % RCF	101.2	2.1×10^{7}	4.2×10^{7}
PC/ABS (60/40) alloy + 15 wt % RCF	115.8	2×10^{7}	3.4×10^{7}
PC/ABS (60/40) alloy + 20 wt % RCF	132.6	1.9×10^{7}	2.8×10^{7}

modulus and high temperature stiffness with increasing temperature. This was also contributed to the enhancement of the HDTs of these composites. Consequently, the improvement in the HDTs of the composites resulted from their enhanced flexural modulus as well as the increased ability to retain high stiffness induced by the fibers or fillers. Nielsen and Landel[42] proposed that the variation of the HDT was related to the flexural behaviors, especially the flexural modulus of polymer compounds with various fillers. In this work, the significant improvement of HDT may be due to the continual increase in the modulus of PC/ABS composites with increasing RCF loading. To achieve a high HDT, the ability of a thermoplastic composite to retain stiffness and modulus with increasing temperature is highly necessary. The incorporation of RCF makes it possible for PC/ABS alloys to maintain a high modulus as well as a high stiffness with an increasing of testing temperature. And the higher the RCF loading, the higher the flexural modulus when set at a high temperature. Thus, such an enhancement of flexural modulus results in an achievement of high HDTs for PC/ABS composites. This result is in good agreement with Nielsen's prediction. Additionally, the RCF acts as a heterogeneous network in the matrix, which can limit the motion of the macromolecular chains and thus prevent the elastic and plastic deformations of the matrix at a higher temperature.

Electrical Resistivity

Considering the excellent electrical conductivity of carbon fibers in nature, it is desired that the incorporating RCF can create a type of conducting thermoplastic composites based on PC/ABS alloys. The volume resistivity and surface resistivity of PC/ABS composites were measured and are summarized in Table II. A steep decrease in electrical resistivity can be observed for the composites at a RCF loading of 5 wt %. Both volume resistivity and surface resistivity are further reduced with increasing the RCF loading, and however, such a decrement is not so significant. These results indicate the formation of intrinsic fibrous structure throughout the PC/ABS matrix. Since the percolation threshold does not appear for the composites with the RCF loading up to 20 wt %, the conductivity mechanism still belongs to tunneling or hopping of charges between separated fibers.[43] In addition, it is noteworthy that the electrical resistivity is also influenced by the fraction of ABS in the alloys, and the higher the ABS content, the lower the volume and surface resistivity. As is well known, PC has a high melt viscosity. The higher fraction of ABS imparts a much better fluidity for the melts, which favors the dispersion of RCF in the polymer matrix. Consequently, more homogenous distribution of RCF in the matrix enhances the conductivity of the composites. Summarily, the significant decrease in electrical resistivity provides electrostatic discharge for the PC/ABS thermoplastic composites. Furthermore, the RCF-reinforced PC/ABS composites are also well balanced in respect to the electronic and mechanical properties due to the notably reinforcing effect of RCF.

Morphology of Fracture Surface

Figure 1 shows the SEM micrographs of the fracture surface obtained from the notched impact tests of PC/ABS composites. These composites are observed to display a great amount of broken fibers as well as a few holes due to the fiber pull-out. With increasing the RCF loading, the fracture surfaces seem to present a feature of major fiber breakage with a few fibers pulling out as shown in Figure 1(c–h), indicating that the impact energy was dissipated mainly by the fiber breakage as well as the partial fiber pull-out. It is interestingly observed from the close-up view that some of fibers are well covered with the polymeric resins in the local area of the fracture surface as seen in Figure 2. The surfaces of these fibers look like roughness and seem to be trapped by an irregular resin layer with linking the fiber surface to the matrix. Such a characteristic morphology is also an indication of the good interfacial bonding between RCF

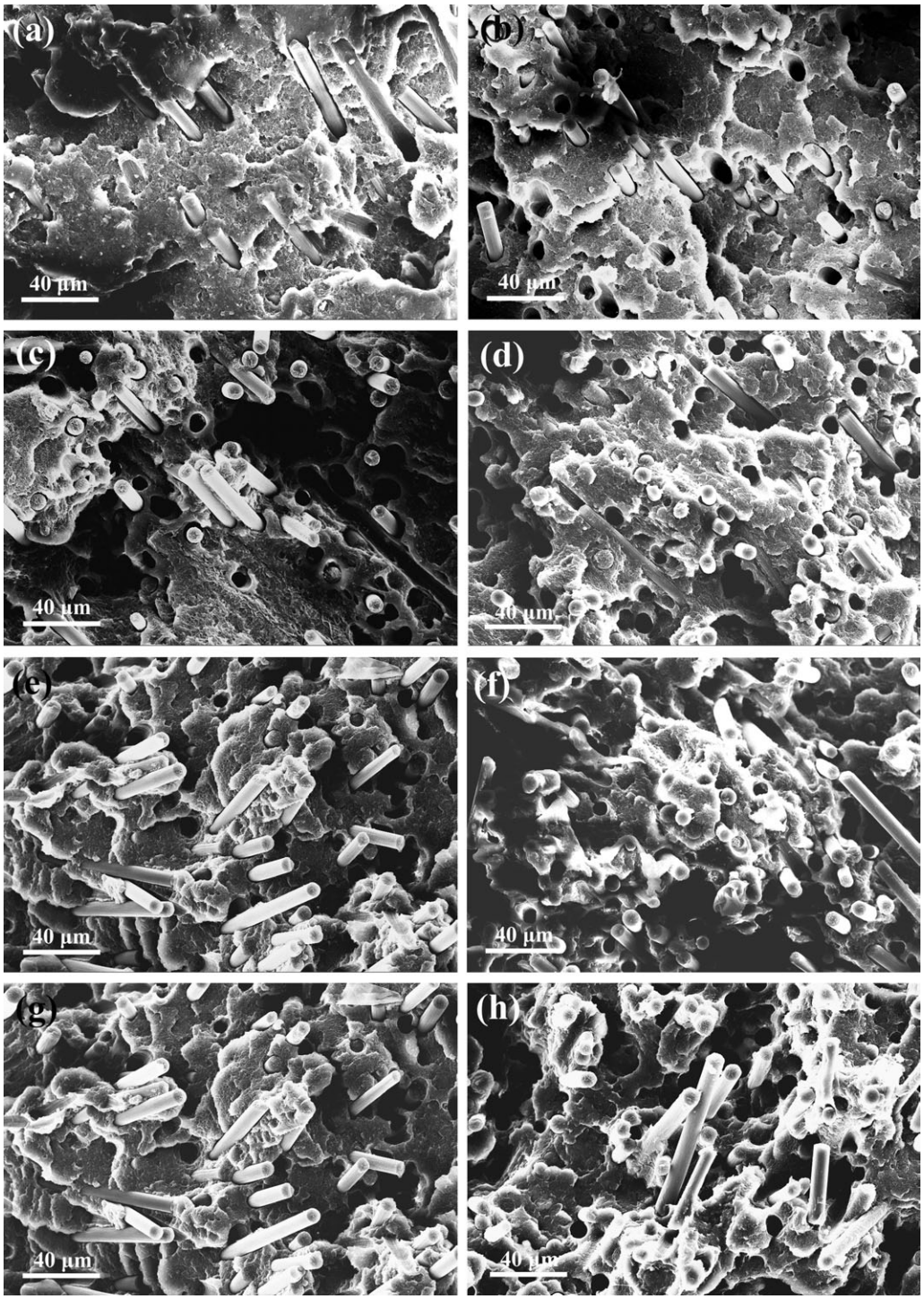

Figure 1. SEM micrographs of impact fracture surfaces for RCF-reinforced PC/ABS composites: (a) PC/ABS (80/20) composites with 5 wt %, (b) 10 wt %, (c) 15 wt %, and (d) 20 wt % of RCF; (e) PC/ABS (70/30) composites with 15 wt % and (f) 20 wt % of RCF; (g) PC/ABS (60/40) composites with 15 wt %, and (h) 20 wt % of RCF.

and PC/ABS matrix, and thus, the better stress transfer can be expected. Additionally, it is also found from the SEM micrographs that ABS is homogeneously dispersed in the PC domain as a very small particle, and most of fibers are well dispersed as individual ones in the matrix. This phenomenon implies that the RCF is mainly distributed in the PC phase, and the coupling agent causes a better wetting of RCF through the PC domain. Such an enhanced interfacial adhesion leads to a significant improvement in tensile and flexural properties. It should also be noted in the SEM micrographs that most of the fibers on the fracture surface were orientated in the flowing direction of injection molding. This indicates that composites have higher

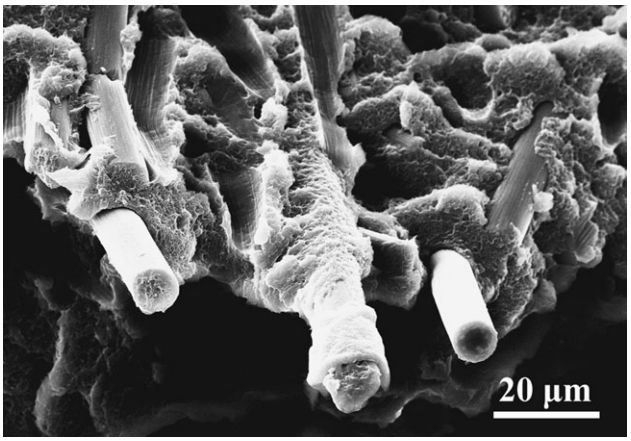

Figure 2. SEM image as a close-up view for the impact fracture surface of PC/ABS (70/30) composites with 15 wt %.

degree of fiber orientation, which results in a higher fiber-efficiency factor and, hence, higher mechanical strength. On the other hand, the impact energy could also be dissipated efficiently via fiber pulling-out, interface debonding, and matrix deforming. It is clearly observed that, in most cases, the fibers are finely dispersed in the PC/ABS matrix; however, a slight aggregation occurs for the composites with high RCF loading as displayed in Figure 1(c–g). In addition, the local matrix deformation occurring near the fibers can be observed in Figure 1, suggesting that the matrix continuity was destroyed; thus, the crack propagation was inhibited. This also leads to a significant improvement in impact toughness of RCF-reinforced PC/ABS composites.

Thermogravimetric Analysis

TGA was used to investigate the thermal stabilities of RCF-reinforced PC/ABS composites. The characteristic degradation parameters obtained from TGA are summarized in Table III. The PC/ABS alloys and their composites are all observed to reveal a typical one-step degradation during their thermal decompositions, indicating that the random scission of the main chains of PC and ABS resins occurred in the close temperature range as the prevailing decomposition reaction. The virgin PC/ABS alloys display the variable initial decomposition temperatures ranging from 370 to 397°C at a weight loss of 3 wt %, which is defined as a onset decomposition temperature (T_{onset}) and, furthermore, taken as an index of thermal stability. The main degradation of these PC/ABS alloys started at a maximum decomposition temperature (T_{max}) around 427–447°C, at which the weight loss occurred at a maximum rate. These two characteristic temperatures are associated with the essential thermal stability of the alloys determined by the weight ratio of PC and ABS in the compounding composition and, afterward, indicate a better thermal stability for the PC/ABS alloy at a weight ratio of 70/30 due to the intrinsic compatibility feature of two phases. It is interesting to note that the PC/ABS composites show slightly lower T_{onset}s than virgin PC/ABS alloys as shown in Table III. This result may be due to the poor thermal stability of the DGEBA resin coated on the surface of RCF. However, all of the composites exhibit higher T_{max}s than the virgin alloys, indicating the enhancement of thermal stability by the addition of RCF. Furthermore, the RCF at a high loading level can effectively act as physical barriers to hinder the transport of volatile decomposed products out of the PC/ABS composites during thermal decomposition; thus, the composite containing 20 wt % RCF exhibits a much higher decomposition

Table III. Thermal Analysis Results Obtained from TGA Measurements for the PC/ABS Alloys and Their Composites with RCF

Sample	Characteristic temperature		Char yield at 750°C (wt %)
	T_{onset}[a] (°C)	T_{max}[b] (°C)	
PC/ABS (80/20) alloy	380.8	437.6	9.48
PC/ABS (80/20) alloy + 5 wt % RCF	377.5	440.5	25.15
PC/ABS (80/20) alloy + 10 wt % RCF	369.8	441.6	30.79
PC/ABS (80/20) alloy + 15 wt % RCF	379.2	445.3	33.61
PC/ABS (80/20) alloy + 20 wt % RCF	378.4	443.6	38.92
PC/ABS (70/30) alloy	397.1	447.3	15.35
PC/ABS (70/30) alloy + 5 wt % RCF	396.3	449.8	20.51
PC/ABS (70/30) alloy + 10 wt % RCF	395.6	450.2	28.25
PC/ABS (70/30) alloy + 15 wt % RCF	398.1	452.6	37.19
PC/ABS (70/30) alloy + 20 wt % RCF	392.5	451.3	42.90
PC/ABS (60/40) alloy	371.6	427.8	9.73
PC/ABS (60/40) alloy + 5 wt % RCF	370.2	426.9	16.01
PC/ABS (60/40) alloy + 10 wt % RCF	368.4	428.3	25.95
PC/ABS (60/40) alloy + 15 wt % RCF	369.8	428.5	30.71
PC/ABS (60/40) alloy + 20 wt % RCF	367.7	429.2	39.15

[a]The onset decomposition temperature, at which the sample undergoes 3 wt % of weight loss.
[b]The characteristic temperature, at which the maximum rate of weight loss occurs.

temperature than the other composite samples. In addition, the char yields of the PC/ABS composites with high RCF loadings are much higher than those with low ones. This result is ascribed to the flame retardancy and carbonization of RCF toward the PC/ABS matrix.[44] Similarly, the RCF also has a good barrier effect on the thermal degradation process, leading to the retardation of the weight loss of thermal degradation products as well as the thermal insulation of the PC/ABS matrix. Consequently, a high char yield was obtained at the end of the thermal decomposition of the RCF-reinforced PC/ABS composites.

Dynamic Mechanical Properties

The dynamic mechanical properties of the RCF-reinforced PC/ABS composites were investigated by dynamic mechanical analysis (DMA), which also reflected the viscoelastic behaviors of these composites in the different compounding compositions. Figures 3 and 4 demonstrate the temperature dependence of storage modulus and loss factor (tan δ) for PC/ABS alloys and their composites with RCF, respectively. The dynamic mechanical behaviors of neat PC and ABS resins are also presented as references in these two figures. The PC/ABS alloys were observed to exhibit slightly lower storage moduli than either PC or ABS at three different weight ratios. However, the incorporation of RCF into PC/ABS alloys significantly improved the storage moduli of the PC/ABS composites. This result is consistent with the tensile and flexural moduli and, thus, can be attributed to the stiffening effect of RCF and the enhanced interfacial interaction between the fibers and the matrix. These two factors may contribute together to the improvement in resilience of the PC/ABS composites.[45,46] Therefore, the PC/ABS composites achieved a successive improvement in storage modulus with increasing the RCF loading. It is also noteworthy that the increment of storage modulus is dependent on the weight ratio of PC and ABS, and the PC/ABS composite at a weight ratio of 60/40 displays a greater increment in storage modulus than the other two composites. This phenomenon is due to the fact that the increase of fraction of ABS enhances the viscoelasticity of PC/ABS matrix because of the much more flexible chains of ABS resin than PC.

The loss factor was found to present a maximum value when all of the samples were heated through the glass transition region in DMA tests as shown in Figure 4. The temperature at the peak corresponding to the maximum tan δ is considered as a glass transition temperature (T_g). Furthermore, the appearance of single tan δ peak of the PC/ABS alloys is an indication of the miscible compounding systems. It is also found that the T_gs of PC/ABS alloys decrease slightly with increasing the fraction of ABS. However, the temperature at the tan δ peak seems not to be significantly affected in the presence of RCF, and the T_g of the PC/ABS matrix seems only to shift to a slightly higher temperature compared to those of virgin PC/ABS alloys. This result can be explained by the fact that the RCF as a rigid filler distributed in the matrix confines the motion of PC and ABS chains. Meanwhile, it is also noted that the presence of RCF in PC/ABS alloys results in a reduction in the height of tan δ peak. It is understandable that the damping in the glass transition zone measures the imperfection in the elasticity and that much of the energy expended for the deformation of a material

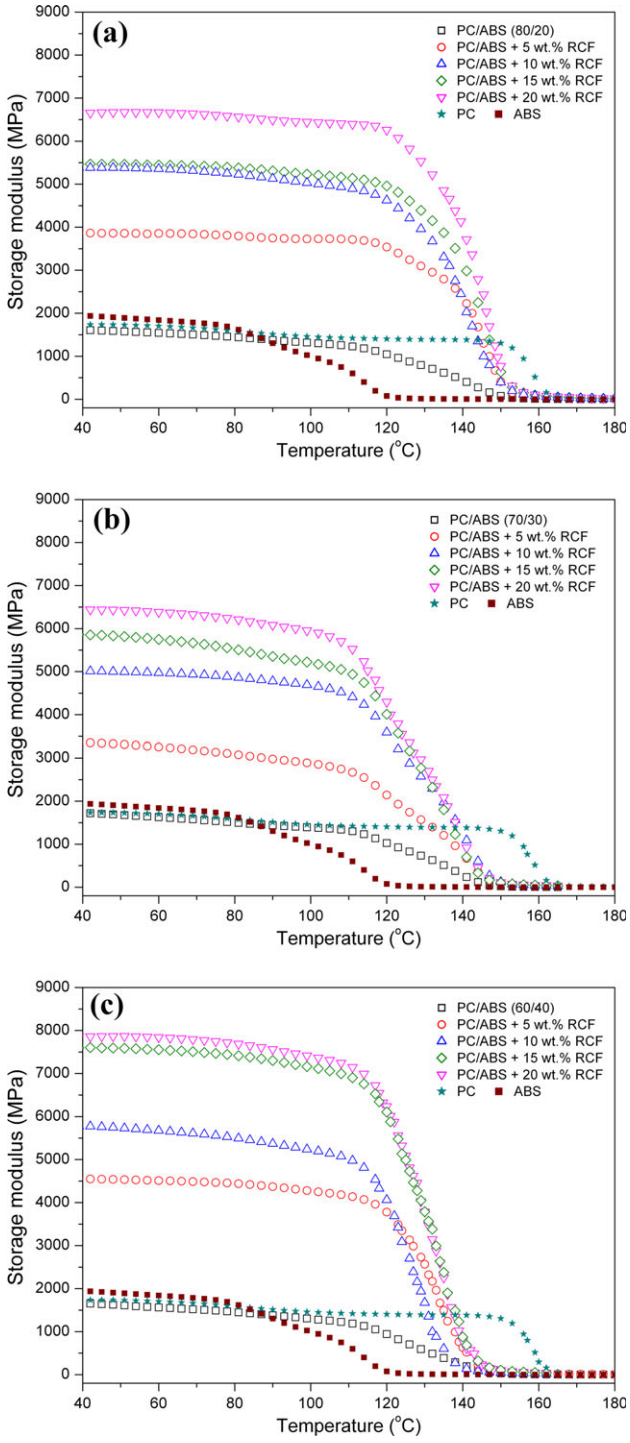

Figure 3. Temperature dependence of storage modulus for RCF-reinforced PC/ABS composites at weight ratios of (a) 80/20, (b) 70/30, and (c) 60/40. [Color figure can be viewed in the online issue, which is available at wileyonlinelibrary.com.]

during DMA testing is dissipated directly into heat.[47] This indicates that the molecular mobility of the composites decreases with the addition of RCF, and thus mechanical loss to overcome inter-friction between molecular chains is reduced. Generally, the damping of the polymer is much greater than that of the

Applied Polymer SCIENCE

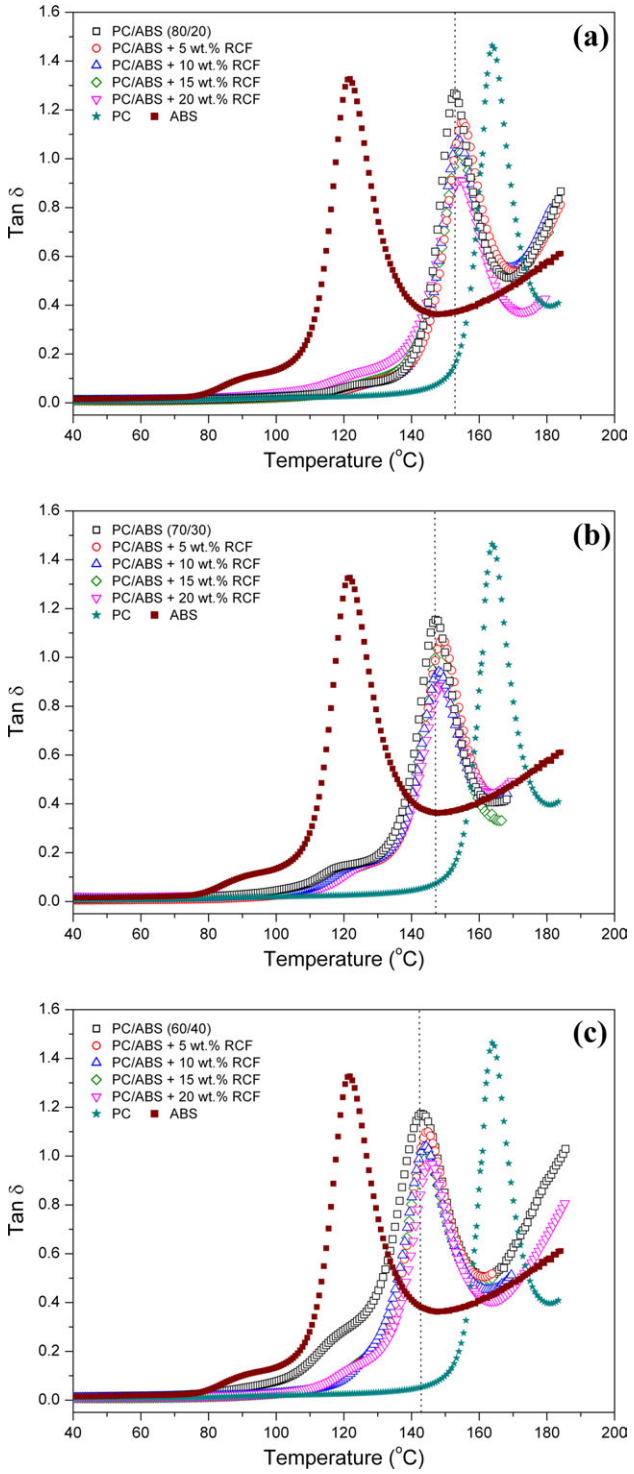

Figure 4. Temperature dependence of loss factor (tan δ) for RCF-reinforced PC/ABS composites at weight ratios of (a) 80/20, (b) 70/30, and (c) 60/40. [Color figure can be viewed in the online issue, which is available at wileyonlinelibrary.com.]

fibers. The introduction of inorganic fibers into polymer matrix will increase its elasticity and reduce its viscosity, and thus, less energy will be consumed to overcome the friction forces between molecular chains.[48] As a result, the loss factor of PC/ABS matrix decreases in the presence of RCF.

CONCLUSION

RCF-reinforced PC/ABS thermoplastic composites were prepared by melting extrusion through a twin-screw extruder. The significant reinforcement effect was achieved for these composites on the basis of the surface treatment for RCF using DGEBA coupling agent, which effectively improved the interfacial bonding between fibers and PC/ABS matrix. As a result, the mechanical properties including tensile strength and modulus, flexural strength and modulus, and notched impact strength were improved significantly. Moreover, the HDT and thermal stability also displayed a prominent improvement by incorporating the surface-treated RCF; meanwhile, the electrical resistivity presented a notable reduction. The SEM micrographs confirmed the fine dispersion of RCF in the PC/ABS matrix and the good interfacial interaction between the fibers and the matrix. In addition, the incorporation of RCF into PC/ABS alloys also led to an increase in the storage moduli of the composites but a decrease in the loss factors. It is prospective that, with such good performance in mechanical data, heat resistance, and electrostatic discharge, the RCF-reinforced PC/ABS composites exhibit a potential application in industrial and civil fields as the high-performance and lightweight materials.

ACKNOWLEDGMENTS

This research was supported by the contract grant sponsor the National Natural Science Foundation of China (contact grant number: 51173010 and 50973005).

REFERENCES

1. Jung, W. H.; Choi, Y. S.; Moon, J. M.; Tortorrela, N.; Beatty, C. L.; Lee, J. O. *Environ. Sci. Technol.* **2009**, *43*, 2563.
2. Wildes, G.; Keskkula, H.; Paul, D. R. *Polymer* **1999**, *40*, 7089.
3. Yin, Z. N.; Fan, L. F.; Wang, T. J. *Mater. Lett.* **2008**, *62*, 2750.
4. Sung, Y. T.; Fasulo, P. D.; Rodgers, W. R.; Yoo, Y. T.; Yoo, Y.; Paul D. R. *J. Appl. Polym. Sci.* **2012**, *124*, 1020.
5. Jeon, S. H.; Kim, H. M.; Park, T.; Choi, B. H.; Choi, W. C. *Mater. Des.* **2011**, *32*, 1306.
6. Bledzki, A. K.; Gajdzik, J. K. *Cell. Polym.* **2010**, *29*, 27.
7. Meier, U. *Struct. Eng. Int.* **1992**, *2*, 7.
8. Gao, Y.; Sun, S.; He, Y.; Wang, X.; Wu, D. *Compos. Part B: Eng.* **2011**, *42*, 1945.
9. Baek, S. J.; Kim, S. Y.; Youn, J. R.; Kim, K. W. *Fiber Polym.* **2011**, *12*, 927.
10. Mizoguchi, M.; Umemura, T.; Takasima, S.; Otsuki, S.; Yang, B. Kuriyama, T.; Leong, Y. W.; Hamada, H. *Polym. Polym. Compos.* **2008**, *16*, 27.
11. Luo, X.; Chung, D. D. L. *Compos. Part B: Eng.* **1999**, *30*, 227.

12. Chiang, W. Y.; Chiang, Y. S. J. *Appl. Polym. Sci.* **1992**, *46*, 673.
13. Rosato, D. V. *Composites* **1973**, *17*, 208.
14. Reh, A.; Plank, B.; Kastner, J.; Gröller, E.; Heinzel, C. *Eurographics Conference on Visualization (EuroVis)* **2012**, *31*, 1185.
15. Huang, C. Y.; Wu, C. C. *Eur. Polym. J.* **2000**, *36*, 2729.
16. Hine, P. J.; Tsui, S. W.; Coates, P. D.; Ward, I. M. *Duckett, R. A. Compos. Part A: Appl. Sci. Manuf.* **1997**, *28*, 949.
17. Davim, J. P.; Reis, P.; Lapa, V.; Antonio, C. C. *Compos. Struct.* **2003**, *62*, 67.
18. Sharma, S. P.; Lakkad, S. C.; *Compos. Part A: Appl. Sci. Manuf.* **2011**, *42*, 8.
19. Pimenta, S.; Pinho, S. T. *Waste Manage.* **2011**, *31*, 378.
20. Pickering, S. J. *Compos. Part A: Appl. Sci. Manuf.* **2006**, *37*, 1206.
21. Prauchner, M. J.; Pasa, V. M. D.; Otani, S.; Otani, C. *Carbon* **2005**, *43*, 591.
22. Jiang, G.; Pickering, S. J.; Lester, E. H.; Turner, T. A.; Wong, K. H.; Warrior, N. A. *Compos. Sci. Technol.* **2009**, *69*, 192.
23. Jiang, G.; Wong, W. H.; Pickering, S. J.; Rudd, C. D.; Walker, G. S. Proceedings of 7th World Congress for Chemical Engineering; Glasgow, **2005**.
24. Pickering, S. J.; Kelly, R.; Kennerley, J. R.; Rudd, C. D.; Fenwick, N. J. *Compos. Sci. Technol.* **2000**, *60*, 509.
25. Davidson, J. Composites Innovation 2007 Conference Proceedings; Barcelona, **2007**.
26. Ogi, K.; Shinoda, T.; Mizui, M. *Compos. Part A: Appl. Sci. Manuf.* **2005**, *36*, 893.
27. Hyde, J. R.; Lester, E.; Kingman, S.; Pickering, S.; Wong, K. H. *Compos. Part A: Appl. Sci. Manuf.* **2006**, *37*, 2171.
28. Pang, E. J. X.; Chan, A.; Pickering, S. J. *Compos. Part A: Appl. Sci. Manuf.* **2011**, *42*, 1406.
29. Turner, T. A.; Pickering, S. J.; Warrior, N. A. *Compos. Part B: Eng.* **2011**, *42*, 517.
30. Akonda, M. H.; Lawrence, C. A.; Weager, B. M. *Compos. Part A: Appl. Sci. Manuf.* **2012**, *43*, 79.
31. McNally, T.; Boyd, P.; McClory, C.; Bien, D.; Moore, I.; Millar, B.; Davidson, J.; Carroll, T. J. *Appl. Polym. Sci.* **2008**, *107*, 2015.
32. Wong, K. H.; Pickering, S. J.; Rudd, C. D. *Compos. Part A: Appl. Sci. Manuf.* **2010**, *41*, 693.
33. Wong, K. H.; Mohammed, D. S.; Pickering, S. J.; Brooks, R. *Compos. Sci. Technol.* **2012**, *72*, 835.
34. Pimenta S.; Pinho, S. T. *Compos. Struct.* **2012**, *94*, 3669.
35. Cranmer, J. H.; Tesoro, G. C.; Uhlmann, D. R. *Ind. Eng. Chem. Prod. Res. Dev.* **1982**, *21*, 185.
36. Jakeways, R.; Smith, T.; Ward, I. M.; Wilding, M. A. *J. Polym. Sci. Part C: Polym. Lett.* **1976**, *14*, 41.
37. Liang, J. Z. *Polym. Test.* **2011**, *30*, 749.
38. Shiao, M. L.; Nair, S. V.; Garrett, P. D.; Pollard, R. E. *Polymer 35*, 306.
39. Wong, A. C. Y. *Compos. Part B: Eng.* **2003**, *34*, 199.
40. Akutsu, F.; Inoki, M.; Inagawa, T.; Kasashima, Y.; Sononda, Y.; Marushima, K. J. *Appl. Polym. Sci.* **1999**, *74*, 1366.
41. Saha, N.; Basu, D.; Banerjee, A. N. J. *Appl. Polym. Sci.* **1999**, *71*, 541.
42. Nielsen, L. E.; Landel, R. F. Mechanical Properties of Polymers and Composites, 2nd ed.; Marcel Dekker: New York, **1994**.
43. Vilcakova, J.; Saha, P.; Quadrat, O. *Eur. Polym. J.* **2002**, *38*, 2343.
44. Lu, H.; Wilkie, C. A. *Polym. Degrad. Stab.* **2010**, *95*, 564.
45. Mukherjee, M.; Das, T.; Rajasekar, R.; Bose, S.; Kumar, S. *Das, C.K. Compos. Part A: Appl. Sci. Manuf.* **2009**, *40*, 1291.
46. Song, L.; Qiu, Z. *Polym. Adv. Technol.* **2011**, *22*, 1642.
47. Huda, M. S.; Drzal, L. T.; Mohanty, A. K.; Misra, M. *Compos. Sci. Technol.* **2006**, *6*, 1813.
48. Chua, P. S. *Polym. Compos.* **1987**, *8*, 308.